Optical properties of an Er^{3+}-doped phosphate glass waveguide formed by single-energy H^+ ion implantation*

CHEN Jing-yi (陈静怡)[1], **YAN Sen** (严森)[1], **ZHENG Rui-lin** (郑锐林)[1], **ZHANG Liao-lin** (张料林)[2], **GUO Hai-tao** (郭海涛)[3], **and LIU Chun-xiao** (刘春晓)[1]**

1. *College of Electronic and Optical Engineering, Nanjing University of Posts and Telecommunications, Nanjing 210023, China*
2. *School of Material Science and Engineering, Jiangxi University of Science and Technology, Ganzhou 341000, China*
3. *State Key Laboratory of Transient Optics and Photonics, Xi'an Institute of Optics and Precision Mechanics, Chinese Academy of Sciences, Xi'an 710119, China*

(Received 20 June 2018; Revised 21 August 2018)

In this work, we report the fabrication of an optical waveguide by single-energy H^+ ion implantation in the Er^{3+}-doped phosphate glass. The ion implantation conditions are with energy of 0.4 MeV and a fluence of 8.0×10^{16} ions/cm^2. The dark mode spectrum of the waveguide structure was measured by the prism coupling experiment. The refractive index change along with the penetration depth was fitted by using the reflectivity calculation method (RCM). Finally, the calculated near-field light intensity distribution shows superior waveguide properties, which demonstrates its promising potentials for compact optical integrated devices.

Document code: A **Article ID:** 1673-1905(2019)02-0104-4

DOI https://doi.org/10.1007/s11801-019-8103-8

The investigations on the preparation and properties of high quality optical waveguides have always been favored by more and more researchers[1-5]. Various techniques, including diffusion of metal materials[6], ion exchange[7], ion implantation[8], femtosecond-laser micromachining[9], have been applied to manufacture optical waveguides on different kinds of materials. Among them, ion implantation has attracted more and more attention owing to its accurate control of both penetration depth and doping element by use of a particular species, as well as the energy of the ions[10]. At the end of the ion trajectory, the nuclear energy deposition of the irradiated ions during the implantation process induces a damaged layer in the optical target material[11]. It leads to the decrease in physical density by means of volume expansion, with a consequent reduction of the refractive index[12].

One of the key issues of waveguide preparation is the selection of a suitable matrix material[13-15]. The Er^{3+}-doped phosphate glass is considered as a type of promising candidate material for the formation of photonic devices mainly because of its isotropic refractive index, good optical transparency in the visible and near-infrared regions and high gain at about 1 550 nm[16,17]. Er^{3+}-doped phosphate glass waveguides have been manufactured by using the technique of ion implantation. In 2016, Chen et al fabricated a waveguide structure in Er^{3+}/ Yb^{3+} co-doped phosphate glass by the swift heavy ion irradiation[18]. In 2017, the proton implantation with energy of (500+550) keV and fluence of $(1.0+2.0)\times10^{16}$ ions/cm^2 was employed to construct an optical waveguide in the Er^{3+}-doped phosphate glass[19]. Obviously, it was double-step. Compared with the double-energy implantation, the single-energy irradiation is simplified. However, a single-energy proton-implanted Er^{3+}-doped phosphate glass waveguide has not been reported so far to the best of our knowledge. In this work, the single-energy proton implantation with energy of 0.4 MeV and a fluence of 8.0×10^{16} ions/cm^2 was carried out for the formation of an optical waveguide in the Er^{3+}-doped phosphate glass. After the implantation of protons, the energy loss distribution of the implanted ions and the optical characteristics of the waveguide were investigated in detail.

The Er^{3+}-doped phosphate glass was provided by Jiangxi University of Science and Technology in the form of a wafer with a thickness of 1.0 mm. The glass was cut into rectangular parallelepipeds with sizes of 8.0 mm×4.0 mm×1.0 mm. It was optically polished by the solution that was made up of amorphous silica, ethylene glycol and formaldehyde. Finally, the phosphate glass was attentively cleaned with acetone, alcohol, and deionized water in turn.

The profile of the nuclear energy loss induced by the ion beam in the Er^{3+}-doped phosphate glass could be calculated by the SRIM-2013 code (stopping and range

* This work has been supported by the National Natural Science Foundation of China (Nos.11405041 and 61505084), and the Natural Science Foundation of Jiangsu Province (No.BK2015084).

** E-mail: chunxiaoliu@njupt.edu.cn

of ions in matter)[20]. For a waveguide fabricated by ion implantation, its thickness depends on the implanted energy, and the refractive index change is decided by the irradiated fluence. The energy of the ions is chosen to be 0.4 MeV based on the desired thickness of the Nd:CNGG waveguide. The fluence of the protons of 8.0×10^{16} ions/cm^2 is selected in consideration of the damage ratio. Therefore, a 400-keV hydrogen ion implantation with a fluence of 8×10^{16} ions/cm^2 was carried out on one of 8.0 mm×4.0 mm surfaces of the Er^{3+}-doped phosphate glass to construct an optical waveguide structure. The irradiation experiment was done on an ion-implantor of Nanaln at room temperature.

The *m*-line spectrum was measured by the prism coupling technique. In the Metricon 2010 prism coupler system, a light beam with a wavelength of 632.8 nm was incident onto the high refractive index prism. A pneumatic coupling head driven by the nitrogen pressure made the waveguide in close contact with the prism. A detector was fixed next to the prism to detect the intensity of light reflected from the prism.

After polishing, the refractive index of the Er^{3+}-doped phosphate glass was measured by the Metricon Model 2010 Prism Coupler. Fig.1 shows the relative intensity of light as a function of the effective refractive index. As one can see, the refractive indices are 1.536 2 and 1.521 7 at wavelengths of 632.8 nm and 1 539 nm, respectively.

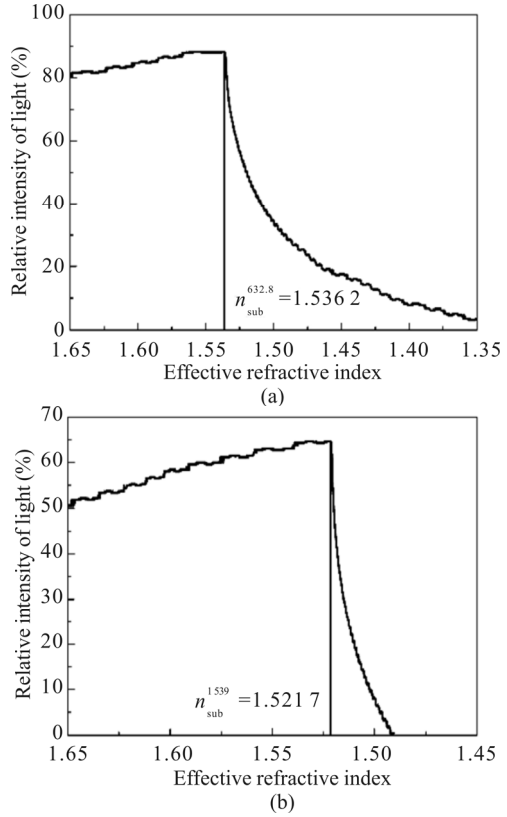

Fig.1 Refractive indices of the Er^{3+}-doped phosphate glass at (a) 632.8 nm and (b) 1 539 nm

When energetic protons were implanted into the Er^{3+}-doped phosphate glass, the H^+ ions lost their energy owing to collisions with nuclei and electrons in the Er^{3+}-doped phosphate glass, resulting in a change in the refractive index of the implanted region. To investigate the relationship between the nuclear energy loss and the penetration depth, the SRIM 2013 program was adopted to simulate the energy deposition process of the 0.4-MeV H^+ ion implantation into the Er^{3+}-doped phosphate glass, as shown in Fig.2. The nuclear energy loss remained nearly zero in the first 0—3 μm and climbed to a maximum value of 1.93 keV/μm at a depth of 4.03 μm. It leads to an optical barrier that could be controlled by the mass, charge and energy of the ions.

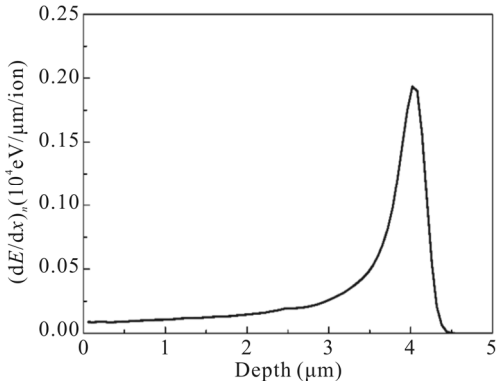

Fig.2 Nuclear energy loss of the 0.4-MeV H^+ ion implantation into the Er^{3+}-doped phosphate glass

Fig.3 shows the cross section of the waveguide structure fabricated by 0.4-MeV H^+ ion implantation with a fluence of 8×10^{16} ions/cm^2 in the Er^{3+}-doped phosphate glass. It was captured by a microscope with 1 000× magnification. In Fig.3, a strip in different colors is the waveguide core layer. Its width is about 4 μm, which is approximately consistent with the ion projected range calculated by the SRIM 2013 code in Fig.2.

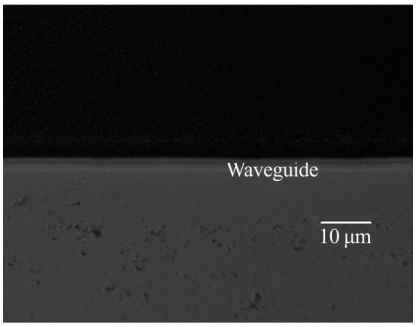

Fig.3 Cross-sectional view of the Er^{3+}-doped phosphate glass waveguide

The propagating modes and their effective refractive indices were recorded by the *m*-line technique. During the measurement process, the light was coupled into the waveguide at certain incident angle. Then a dip was present in the dark-mode spectrum, which could be called a guided mode. Fig.4 illustrates the *m*-line curve for the Er^{3+}-doped phosphate glass implanted by 0.4-MeV pro-

tons with a fluence of 8×10^{16} ions/cm^2. There are a total of two dips in Fig.4. The second dip is wide and may correspond to a leaky mode. However, the first dip is sharp and can be considered as a true guided mode (TE_0 mode). The incident angle (θ), the refractive index of the prism (n_p), and the effective refractive index of the mode (n_{eff}) have a function of $n_{eff}=n_p\sin\theta$. The effective refractive index of the first mode (1.527 6) is lower than the substrate refractive index (1.536 2), suggesting an optical barrier-type waveguide.

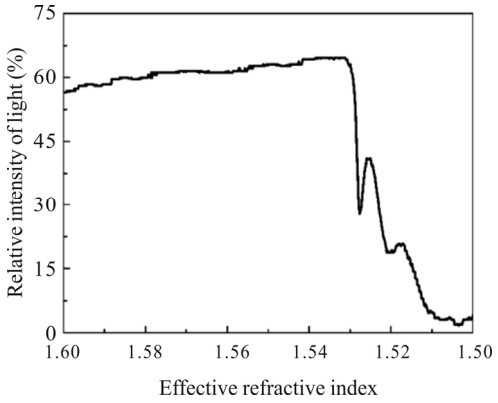

Fig.4 TE dark mode spectrum of the proton-implanted Er^{3+}-doped phosphate glass waveguide at 623.8 nm

The refractive index distribution is an important parameter for an optical waveguide structure. It has an impact on the propagation modes. The index profile of the proton-implanted Er^{3+}-doped phosphate glass waveguide was calculated by means of the reflectivity calculation method (RCM) that consisted of two half-Gaussian curves[21], as shown in Fig.5. A decrease of 0.007 in the refractive index occurred in the region from the glass surface to 3.64 μm. On the other hand, an optical barrier with a minimum refractive index of 1.516 2 was located at 4.01 μm below the surface of the Er^{3+}-doped phosphate glass. Therefore, the waveguide layer was expected to be fabricated in the region between the optical barrier and the glass surface. It can be seen from Tab.1 that the effective refractive indices obtained by the RCM are close to the experimental ones. Therefore, the final function curve in the process of the RCM simulation can accurately describe the refractive index distribution of the waveguide.

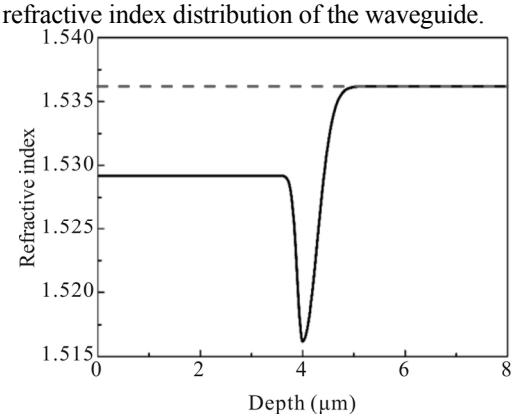

Fig.5 Refractive index as a function of the penetration depth for the fabricated waveguide

Tab.1 Comparison of the measured and calculated effective refractive indices for the Er^{3+}-doped phosphate glass waveguide formed by the proton implantation

Mode	Effective refractive index		
	Exp.	Cal.	Diff.
TE_0	1.527 6	1.527 577 58	2.242×10^{-5}
TE_1	1.520 6	1.522 582 57	$-1.982\ 57\times10^{-3}$

The finite-difference beam propagation method (FD-BPM) is a common way for the calculation of the modal distributions for a number of optical waveguides[22-24]. Fig.6 shows the simulated near field intensity distribution for the TE_0 mode of the proton-implanted Er^{3+}-doped phosphate glass waveguide. As can be seen, most of light is inside the waveguide core. Therefore, the planar optical waveguide can support the fundamental TE_0 mode for 632.8 nm. Moreover, the computed effective refractive index of the TE_0 mode by the FD-BPM is 1.527 577, which is in agreement with the counterpart in the *m*-line spectrum.

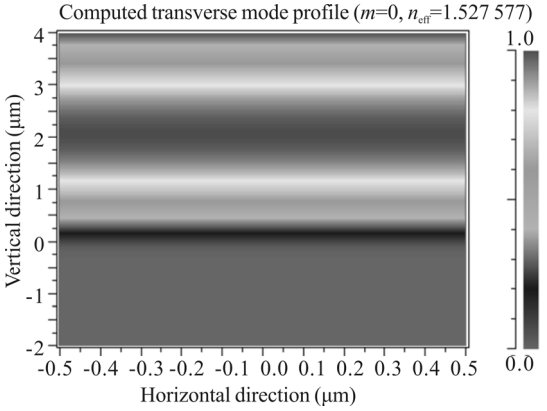

Fig.6 Simulated near field intensity distribution for the proton-implanted waveguide

Ion implantation has been extensively used to fabricate optical waveguides with stability and compactness. Er^{3+}-doped phosphate glass plays a necessary role in the formation of photonic elements. In this work, planar Er^{3+}-doped phosphate glass waveguides have been configured by the proton implantation at energy of 0.4 MeV and a dose of 8×10^{16} ions/cm^2. Based on the microscope image, a distinguished waveguide layer with a thickness of 4.0 μm is present in cross-section. The prism-coupling measurement indicates that there is a guided mode and a leaky mode in the waveguide structure. Compared with the unimplanted glass, the refractive indices in the waveguide region and the optical barrier region are reduced by 0.007 and 0.02, respectively. The optical waveguide has a promising light confinement effect, according to the FD-BPM simulation. In view of the above experimental data, the ion-implanted Er^{3+}-doped phosphate glass waveguides can emerge as candidates for efficient and compact active devices.

References

[1] Zhang Mian, Wang Cheng, Rebeca cheng, Shams-Ansari Amirhassan and Loncar Marko, Optica **4**, 1536 (2017).

[2] Ríos Carlos, Stegmaier Matthias, Hosseini Peiman, Wang Di, Scherer Torsten, Wright C. David, Bhaskaran Harish and Pernice Wolfram H. P., Nature Photonics **9**, 725 (2015).

[3] Wang Lei, Haunhorst Christian E., Volk Martin F., Chen Feng and Kip Detlef, Optics Express **23**, 30188 (2015).

[4] Ma Li-Nan, Tan Yang, Ghorbani-Asl M., Boettger R., Kretschmer S., Zhou S., Huang Z., Krasheninnikov A. V. and Chen Feng, Nanoscale **9**, 11027 (2017).

[5] Wang Xue-Lin, Chen Feng, Wang Ke-Ming, Lu Qing-Ming, Shen Ding-Yu and Nie Rui, Applied Physics Letters **85**, 1457 (2004).

[6] Hu Hui, Ricken R. and Sohler W., Applied Physics B **98**, 677 (2010).

[7] Tervonen Ari, Honkanen Seppo and West Brian R., Optical Engineering **50**, 071107 (2011).

[8] Tan Yang, Zhang C., Chen Feng, Liu Q. F., Jaque D. and Lu Qing-Ming, Applied Physics B **103**, 837 (2011).

[9] Chen Feng and Aldana J. R. Vázquez de, Laser and Photonics Reviews **8**, 251 (2014).

[10] Chen Feng, Laser and Photonics Reviews **6**, 622 (2012).

[11] Vázquez G. V., Valiente R., Gómez-Salces S., Flo res-Romero E., Rickards J. and Trejo-Luna R., Optics and Laser Technology **79**, 132 (2016).

[12] Bányász I., Zolnai Z., Fried M., Berneschi S., Pelli S. and Nunzi-Conti G., Nuclear Instruments and Methods in Physics Research Section B: Beam Interactions with Materials and Atoms **326**, 81 (2014).

[13] Tan Yang, Chen Feng, Wang Lei, Wang Ke-Ming and Lu Qing-Ming, Journal of the Korean Physical Society **52**, S80 (2008).

[14] Wang Yue, Shen Yuan, Zheng Rin-Lin, Shen Jian-Ping, Guo Hai-Tao and Liu Chun-Xiao, Results in Physics **10**, 200 (2018).

[15] Wang Yue, Shen Xiao-Liang, Zheng Rui-Lin, Guo Hai-Tao, Lv Peng and Liu Chun-Xiao, Journal of the Korean Physical Society **72**, 765 (2018).

[16] Bradley Jonathan D. B. and Pollnau Markus, Laser and Photonics Reviews **5**, 368 (2011).

[17] Desirena H., De la Rosa E, Diaz-Torres L. A. and Kumar G. A., Optical Materials **28**, 560 (2006).

[18] Chen Chen, He Rui-Yun, Tan Yang, Wang Biao, Akhmadaliev Shavkat, Zhou Sheng-Qiang, Javier R. Vázquez de Aldana, Hu Li-Li and Chen Feng, Optical Materials **51**, 185 (2016).

[19] Liu Chun-Xiao, Shen Xiao-Liang, Guo Hai-Tao, Li Wei Nan and Wei Wei, Optik **131**, 132 (2017).

[20] Ziegler J. F., SRIM-The Stopping and Range of Ions in Matter, http://www.srim.org.

[21] Chandler P. J. and Lama F. L., Optica Acta **33**, 127 (1986).

[22] Rsoft Design Group, Computer software BeamPROP ver sion 8.0, http://www. rsoftdesign. com.

[23] Tan Yang, Aldana Vázquez de Javier R. and Chen Feng, Optical Engineering **53**, 107109 (2014).

[24] Wang Qing-Yang, Li Xiao-Hui and Zhang Jing-Yu, Optik **164**, 721 (2018).